Hindawi
Advances in Polymer Technology
Volume 2019, Article ID 7143023, 13 pages
https://doi.org/10.1155/2019/7143023

Research Article

Effect of the Nonprestressed/Prestressed BFRP Bar on Flexural Performance of the Bamboo Beam

Qingfang Lv, Yi Ding, and Ye Liu

Key Laboratory of Concrete and Prestressed Concrete Structures of the Ministry of Education, Southeast University, Nanjing 210096, China

Correspondence should be addressed to Ye Liu; 459912879@qq.com

Received 26 March 2019; Accepted 21 August 2019; Published 9 October 2019

Academic Editor: Anil K. Bhowmick

Until now, the systematical and comprehensive strengthening techniques have not been formed for the bamboo structure. Under such background, this paper aims to explore the effects of the application of the nonprestressed and prestressed basalt fiber-reinforced polymer (BFRP) bars on the flexural performance of the beams made of the laminated bamboo and reconstituted bamboo materials. Two series of four-point bending tests were thus conducted. In the first series of tests, the pure laminated bamboo beam and the laminated bamboo beam applied with nonprestressed BFRP bar were compared. Test results showed that the ultimate load and deformation capacity of the laminated bamboo beam was improved due to the existence of the BFRP bar. In the second series of tests, the reconstituted bamboo beams applied with nonprestressed and prestressed BFRP bars were compared. It is found that the ultimate load of the reconstituted bamboo beam was not improved by the application of the prestressed force. The further analysis related to the prestress loss demonstrated that the prestress loss before the release of the prestressed BFRP bar could reach up to 31.8–37.3% compared with the design initial prestressed stress. The prestress loss caused by the elastic deformation of the bamboo beam can be neglected. For all tested specimens, the plane section assumption was acceptable and the position of the neutral axis of the beam gradually moved down with the increase of the applied load.

1. Introduction

The wood, as a typical biological material, has been widely used in civil construction, car industry, furniture industry [1–3], which promotes extensive studies on wood structures [4]. There are still many disadvantages of wood including a long growth, slow regeneration, a significant shortage, and a low utilization rate of the raw materials [5, 6]. Therefore, it is necessary to explore more feasible and appropriate materials similar to the wood, and the bamboo is attracting researchers' attention. Compared with wood, advantages of the bamboo are demonstrated as follows: (1) faster growth speed, (2) high specific strength, (3) high specific rigidity, and (4) lower water swelling ratio [7, 8]. The bamboo can be conveniently obtained in China, which is characteristic as saving costs, environmental friendliness, and recyclability [9–11].

However, the mechanical properties of the raw and unprocessed bamboo material are unstable, with large discreteness [12]. Many inevitable defects can also be found in the unprocessed bamboo material, which results in a poor durability [13–15]. To utilize advantages of the raw bamboo and improve its material stability and performance, kinds of bamboo engineering material, including laminated bamboo [16, 17] and reconstituted bamboo [18, 19], have been proposed and studied, which is beneficial to reduce the material discreteness and enlarge practical applications of the bamboo [7]. Same with the wooden structure, the design of the bamboo structure is often controlled by the structural stiffness [20], which limits the application of the bamboo engineering material and wastes a large amount of strength capacity.

As revealed by many existing investigations on the flexural performance of the bamboo beams, the failure modes of the bamboo beam are mainly featured as the fracture of tensile bamboo fibers and the excessive mid-span deflection under flexural loads. Therefore, to improve the practical utilization of the bamboo engineering material, the strengthening techniques [21–24] are recommended and of important necessity. In the previous studies of wood structures, strengthening

techniques include prestressed steel bar [21], carbon fiber-reinforced polymer (CFPR) sheet [25], glass fiber-reinforced polymer (GFRP) sheet [26] and CFRP bar [27], etc. However, the incompatible elastic moduli of steel and wood resulted in the significant deformation of the wood and large prestress loss [28].

The strengthening techniques for bamboo structures are not systematical and comprehensive compared with wood structures [29]. Wei et al. conducted a series of tests to study the effect of the steel bar and FRP sheet on the flexural performance of the bamboo scrimber beams [29]. Test results showed that the application of the fiber-reinforced polymer can be effective in improving the flexural performance of bamboo beams. Compared with the steel and CFRP, the elastic modulus of the basalt fiber reinforced polymer (BFRP) is relatively small [30], which may have a better cooperative working performance with bamboo engineering material [31]. The analyses on the prestress loss and flexural performance of the laminated bamboo beam applied with prestressed BFRP sheet have already conducted by Lv et al. [32].

Inspired by the above studies, this paper explores the application of the BFRP bar in the laminated bamboo beam and reconstituted bamboo beam. In total, two series of tests were involved in the present study. In the first series, the effect of the application of the nonprestressed BFRP bar on the flexural performance of the laminated bamboo beam was evaluated. In the second series, the effect of the application of the initial prestressed force to the BFRP bar on the flexural performance of the reconstituted bamboo beam was assessed.

2. Material Properties

2.1. Bamboo Engineering Materials. In the present study, the laminated bamboo was composed of bamboo strips and the reconstituted bamboo was fabricated from bamboo fibers. Based on the production process requirements of both bamboo engineering materials, the moso bamboo with the age of 3–5 years was selected. A total of 24 laminated and reconstituted bamboo specimens with the dimension of 30 mm × 30 mm × 45 mm were tested under compression and a total of 24 laminated and reconstituted bamboo specimens with the dimension of 30 mm × 8 mm × 300 mm were tested under tension per Chinese standards [33, 34]. Test results are listed in Table 1.

2.2. BFRP Bar. The geometric shape of the BFRP bar is of importance to the bonding behavior between the BFRP bar and bamboo engineering materials. The purposely designed geometric shape of the BFRP bar is shown in Figure 1. The material properties of the BFRP bar are list in Table 1.

3. Test Program

3.1. Specimen Preparation. The main construction method for the wood beam applied with FRP bar can be featured as: Embed the FRP bar in the groove of the grooved wood beam and then glue them together by epoxy resin or phenolic resin

Table 1: Material properties of bamboo engineering materials and BFRP bar.

Material	σ_{cu} (MPa)	σ_{tu} (MPa)	ε_{tu} (%)	E (GPa)
BSL	97.0 (5.08%)	131.4 (6.43%)		11.6 (3.74%)
BCR	78.1 (6.12%)	181.5 (6.93%)		14.1 (4.31%)
BFRP bar		897.0 (5.51%)	2.75 (6.16%)	32.3 (2.42%)

Note: BSL is the laminated bamboo; BCR represents the reconstituted bamboo; σ_{cu} is the ultimate compressive stress; σ_{tu} is the ultimate tensile stress; ε_{tu} is the ultimate tensile strain; E is the elastic modulus; numbers in the brackets are coefficients of variation (COV).

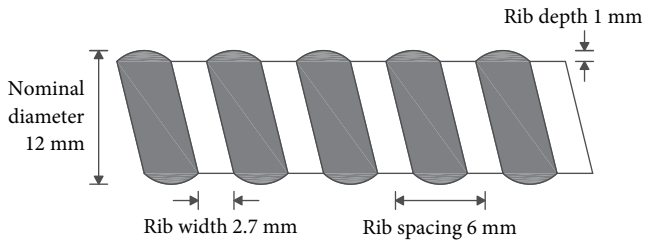

Figure 1: Geometric shape of the BFRP bar.

[31, 35–37]. The above method is suitable for the construction on site but it is relatively complicated, time-consuming, high-price, and material-wasting. In order to respond to the building industrialization advocated by China recently, a once-forming method suitable to the mass production in the factory is adopted in this paper which simplifies the fabrication process of the bamboo beam applied with FRP bar. The once-forming processing technology [38] is summarized for the laminated bamboo beam and reconstituted bamboo beam applied with BFRP bars, respectively: (1) laminated bamboo beam with BFRP bar: stripping, drying, dipping, embedding BFRP bar, parallel assembly, hot pressing, and cutting; (2) reconstituted bamboo beam with BFRP bar: crushing, drying, dipping, embedding BFRP bar, parallel assembly, cold pressing, thermal curing, and cutting. It is obvious that the BFRP bar is embedded in the bamboo beam during the fabrication process. Besides, the BFRP bar is recommended to be embedded in the bamboo beam parallel to the bamboo stripe or the bamboo fiber.

3.2. Method of Prestressing Tension. As shown in Figure 2(a), the steel mould is designed for the bamboo beam, which can also work as the reaction equipment for the prestressing tension system depicted in Figures 2(b) and 2(c). In the bamboo beam applied with prestressed BFRP bar, the prestressing tension system is divided into the tensioned end (see Figure 2(b)) and fixed end (see Figure 2(c)). The main anchorage process for the BFRP bar is summarized as follows: the BFRP bar is firstly placed in the center of a steel tube with inner threads and then the epoxy resin is poured into the steel tube to bond the BFRP bar and steel tube together.

There are three steps involved in the prestressing tension of the BFRP bar: (1) Position the BFRP bar at the bottom of the bamboo beam. The distance between the outer surface of

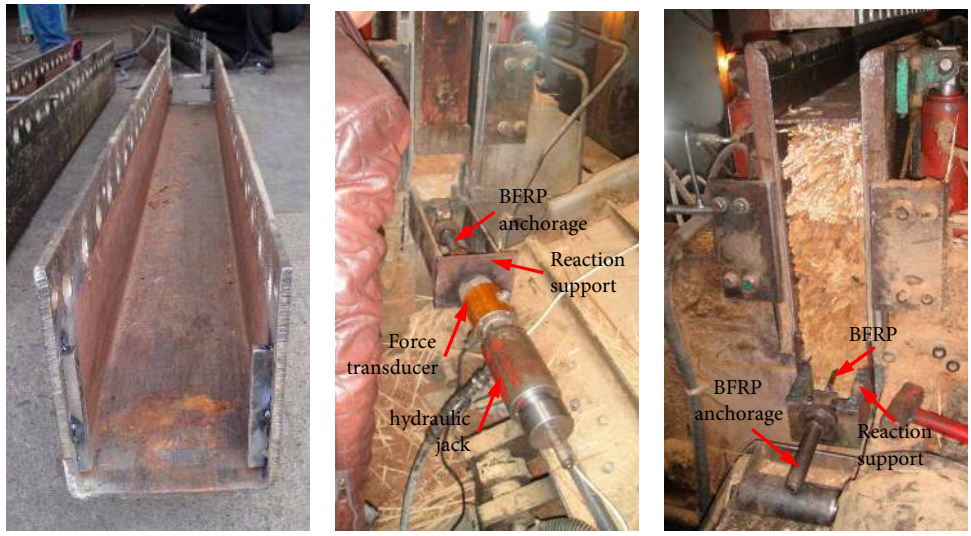

(a) (b) (c)

Figure 2: Prestressing tension system: (a) steel mould for bamboo beam, (b) tensioned end, and (c) fixed end.

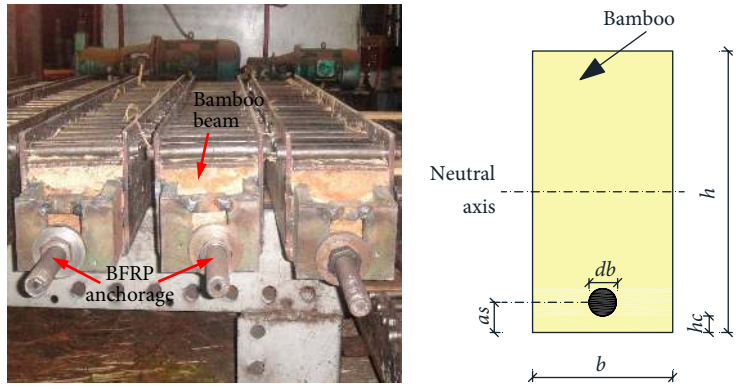

(a) (b)

Figure 3: Sketch of completed specimens: (a) photo and (b) cross-section detail.

the BFRP bar and beam bottom surface is designed as 14 mm, which is also recognized as the cover depth. (2) Apply the initial prestressed force to the BFRP bar. A graded tension method is adopted in the present experimental program until the target initial prestressed force. (3) Press the bamboo beam and release the BFRP bar. After reaching the target initial prestressed force, the bamboo beam is pressed (mentioned in Section 3.1) and then the tensioned end of the prestressing tension system is removed.

3.3. Control of Initial Prestressed Force. The principle of designing the initial prestressed force is to avoid too large initial deformation of the bamboo beam, large bond-slip between the bamboo beam and BFRP bar and creep fracture of the BFRP bar. The design of the initial prestressed force applied to the BFRP bar is analyzed based on above three points.

3.3.1. Control of Initial Prestressed Force. When the initial prestressed force applied to the BFRP bar is large, the bamboo beam may be in the excessive anti-arch state in the normal use state and a too large anti-arch value has a negative effect on the bamboo beam. The recommended initial anti-arch deflection caused by the initial prestressed force of the BFRP bar is defined as $l/500$ based on the principle of the initial anti-arch deflection equal to the deflection resulted from the dead load, where the dead load was taken as 0.15 kN/m^2 and l is the total length of the bamboo beam. For a certain initial prestress level, the calculated initial anti-arch deflection can be compared with the recommended initial anti-arch deflection, $L_t/500$, to determine whether the initial prestress level is appropriate.

When the prestress loss was neglected and the elastic state of the bamboo beam was assumed in the normal use state, the initial anti-arch value, ω_i, of the bamboo beam caused by the initial prestressed force of the BFRP bar is expressed in the following equation:

$$\omega_i = \frac{M_i L_t^2}{8EI}, \tag{1}$$

where M_i is the initial moment caused by the initial prestressed force, F_i, and is expressed in Eq. (2); E is the elastic modulus of the bamboo beam, as listed in Table 1; I equal to $bh^3/12$ is the moment of inertia of the bamboo beam, where b and h are the width and height of the bamboo beam, respectively, as shown in Figure 3(b).

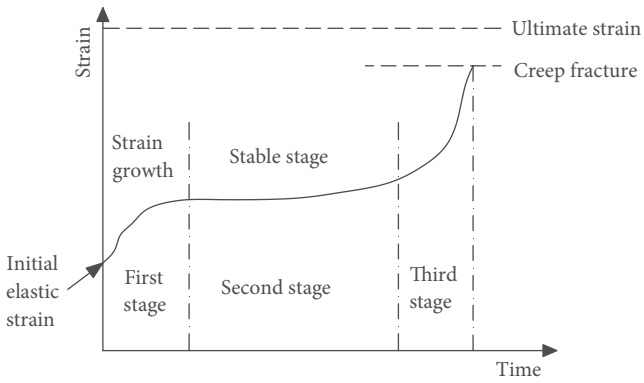

Figure 4: Typical creep curve of the FRP bar.

$$M = f_i A_b \left(\frac{h}{2} - h_c - \frac{d_b}{2} \right), \tag{2}$$

where f_i equal to (F_i/A_b) is the initial prestress stress; A_b assumed as $(\pi d_b^2/4)$ is cross-section area of the BFRP bar; d_b is the nominal diameter of the BFRP bar; h_c is the cover depth, which is 14 mm.

3.3.2. Bond-Slip Verification of the Bamboo Beam with BFRP Bar. Based on previous study [38], the bond strengths, F_{bu}, of the laminated bamboo-BFRP bar composite specimen with a bond length of 90 mm and 300 mm are 17.46 kN and 49.53 kN, respectively. The bond strength of the reconstituted bamboo-BFRP bar composite specimen with a bond length of 124 mm is 24.75 kN. Besides, the bonding between the BFRP bar and reconstituted bamboo is better than the bonding between the BFRP bar and laminated bamboo. In order to avoid the bond slip between the BFRP bar and bamboo beam, the applied initial prestressed force, F_i, should be controlled less than the bond strength, F_{bu}, as expressed in the following equation:

$$F_i \leq F_{bu}. \tag{3}$$

3.3.3. Check of the Creep Fracture of the BFRP Bar. The creep of the BFRP bar can be expected due to the existence of the fiber reinforced resin. The typical creep-time curve of the FRP bar is shown in Figure 4 [39], which can be divided into three stages including the strain growth stage, stable stage and fracture stage. In the creep fracture, the stress level of the BFRP bar at the failure point is less than the ultimate stress of the BFRP bar [40]. Based on test results conducted by Wang et al. [41], the prestressing level of BFRP bar can be determined as 0.52 σ_{tu} to avoid the creep rupture.

3.4. Specimen Details. Two series of tests are adopted in the present study. All BFRP bars employed for the two series of specimens have a nominal diameter of 12 mm. Details of the first series of specimens are listed in Table 2. In the first series, the specimen A0 is a pure laminated bamboo beam without BFRP bar, and the specimen A1 is a laminated bamboo beam applied with BFRP bar but no initial prestressed force is adopted.

Details of the second series of specimens are listed in Table 3. In the second series, the reconstituted bamboo beam applied with BFRP bar is adopted. In order to apply the prestressed force conveniently and safely, the dimension of the reconstituted bamboo beams in the second series was increased compared with the first series of specimens. However, the dimensions of specimens in the second series fluctuated a little because of the fabrication errors. Especially, the relatively large deviation of the value of a_s was observed in the specimens B0, B1, and B2. The measured values of a_s for the three specimens are 13 mm, 24 mm, and 23 mm, respectively, while the design value of a_s should be 20 mm. This phenomenon is explained as follows: The position of the BFRP bar is controlled by fine steel wires in the present study which only provide small restraint for the BFRP bar. During the fabrication of the reconstituted bamboo beam, the position of the BFRP bar is changed under pressing. Therefore, it is necessary to propose a better limit device to control the position of the BFRP bar in the future study. No initial prestressed force is applied to the specimen B0, and the initial prestressed forces of 18.29 kN and 16.73 kN are applied to specimens B1 and B2, respectively.

For specimens B1 and B2, the initial anti-arch deflection, bond slip between the reconstituted bamboo beam and BFRP bar and creep fracture of the BFRP bar should be checked. As listed in Table 3, the calculated initial anti-arch deflections for specimens B1 and B2 are 3.14 mm and 2.87 mm, respectively, which are both less than $l/500$. As discussed above, for the reconstituted bamboo beam-BFRP bar composite specimen with a bond length of 124 mm, the bond strength is 24.75 kN far more than the applied initial prestressed force. Actually, the bond length of the reconstituted bamboo beam applied with BFRP bar is designed as 300 mm, and the bond strength is found to be increased with the increase of bond length. Therefore, the bond slip between the reconstituted bamboo and BFRP bar can be prevented in specimens B1 and B2. Besides, as required in Section 3.3.3, the creep fracture of the BFRP bar can be avoided when the applied initial prestressed force (18.29 kN or 16.73 kN) is less than 101.40 kN $(0.52\sigma_{tu}A_b)$.

3.5. Test Protocol. The four-point bending test was adopted in the present experimental protocol for all specimens, as shown in Figure 5, where a pre-load of 2 kN was applied to the specimen to verify the workability of the equipment. Then, the specimen was loaded at a loading rate of 3 kN/min until failure. The layout of the strain gages and displacement transducers for the first and second series is shown in Figure 6. All data were automatically collected by TDS 530. As depicted in Figure 6, the distances between two supports for the two series of specimens are 1080 mm and 1740 mm, respectively.

4. Test Results and Discussions

4.1. Experimental Observations. First series: For both specimens A0 and A1, the deflection of the laminated bamboo beam slowly increased with the increasing load at the initial loading stage. After the proportional limit, the deflection of the laminated bamboo beam developed quickly. When the applied load approximated the ultimate load, the bamboo

Table 2: Details of tested laminated bamboo beams applied with/without BFRP bar.

Type	Label	$b \times h \times l$ (mm)	d_b (mm)	Fi (kN)	a_s (mm)	Note
Laminated bamboo beam	A0	$30 \times 60 \times 1200$	0			without BFRP bar
	A1		12	0	18	with BFRP bar

Note: d_b is the nominal diameter of the BFRP bar; F_i is the applied initial prestressed force; a_s is the distance between the axis of the BFRP bar and beam bottom surface.

Table 3: Details of tested reconstituted bamboo beams applied with nonprestressed/prestressed BFRP bar.

Type	Label	$b \times h \times l$ (mm)	d_b (mm)	F_i (kN)	a_s (mm)	ω_0 (mm)
Reconstituted bamboo beam	B0	$66.6 \times 120.7 \times 1869$	12	0	13	0
	B1	$60.8 \times 112.5 \times 1865$	12	18.29	24	3.14
	B2	$62.4 \times 113.4 \times 1870$	12	16.73	23	2.87

Note: ω_0 is the calculated initial anti-arch deflection caused by the initial prestressed force based on Eqs. (1) and (2).

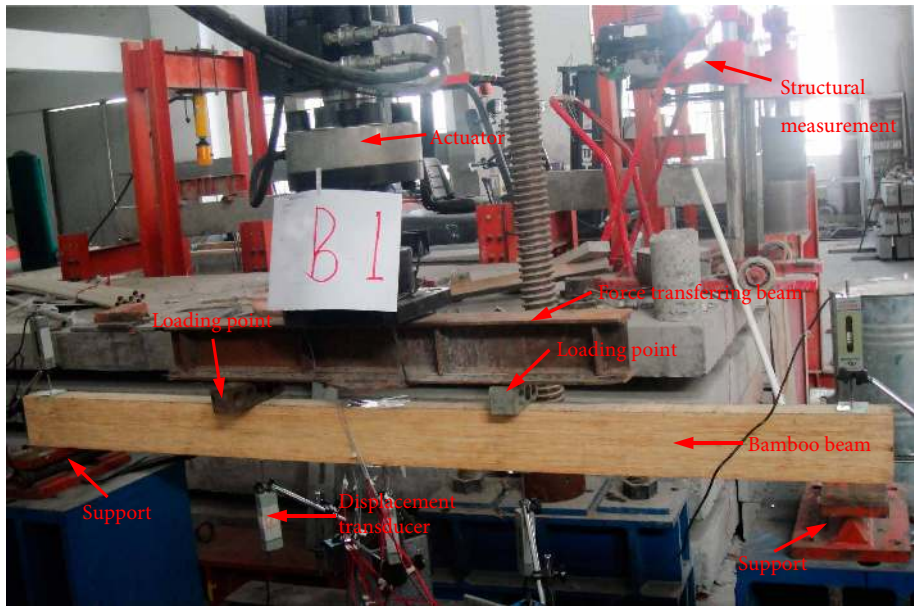

Figure 5: Test setup.

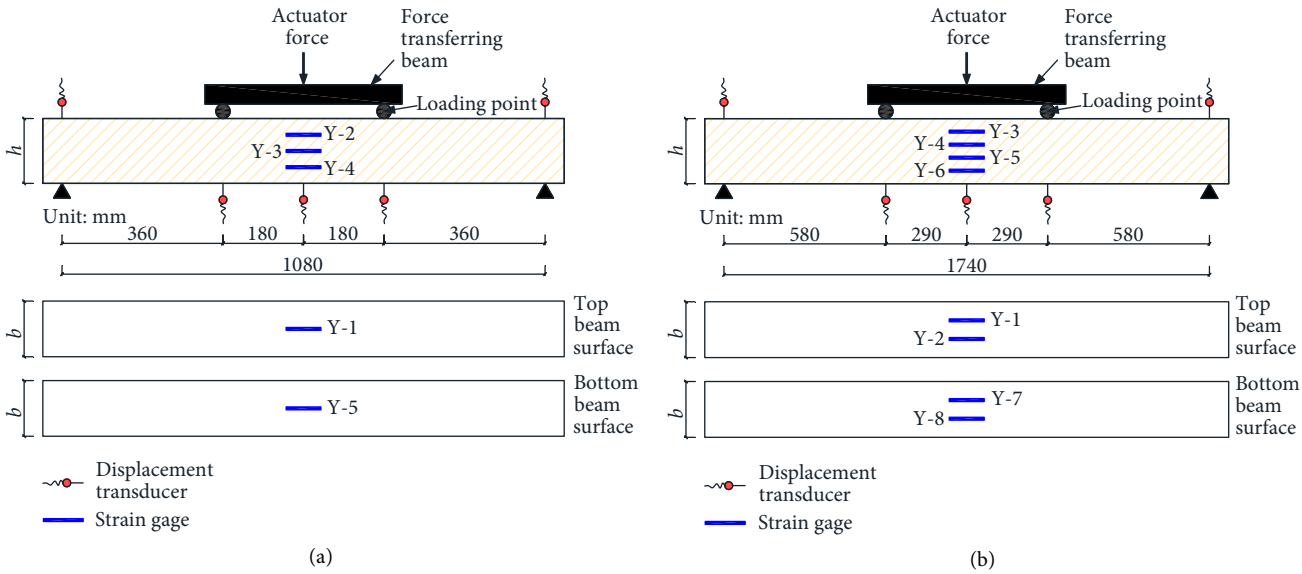

Figure 6: Layout of measurement equipment: (a) first series and (b) second series.

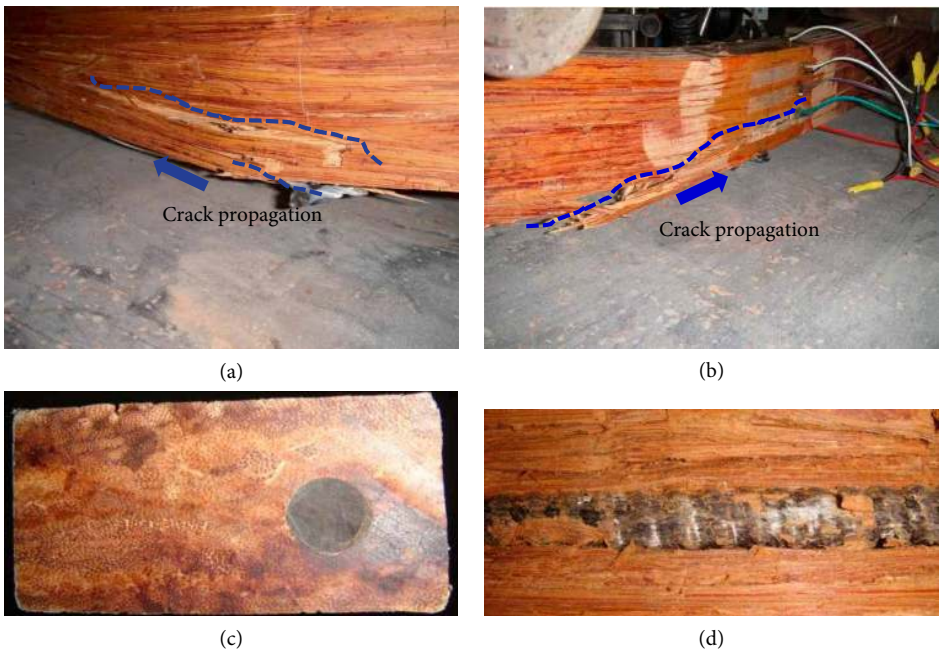

Figure 7: Failure photos: (a) failure position of specimen A0, (b) failure position of specimen A1, (c) end of specimen A1, and (d) the BFRP bar in the middle of the laminated bamboo beam.

fibers gradually fractured, accompanied with small sound. Small cracks initiated from the loading points and propagated to the middle of the laminated bamboo beam, as shown in Figures 7(a) and 7(b).

In specimen A0, the failure of the laminated bamboo beam was accompanied with a loud noise and no more load could be resisted by the laminated bamboo beam, which meant the complete failure of the laminated bamboo beam. In specimen A1, the laminated bamboo beam also fractured at the ultimate load, but the BFRP bar could still work and sustain some part of the load. The strength of the laminated bamboo beam gradually reduced with the further deflection. The test of the specimen A1 was stopped before the complete failure of the laminated bamboo beam when the deflection of the laminated bamboo beam was too large. The failure photos for specimens A0 and A1 in the first series are shown in Figures 7(a) and 7(b).

As shown in Figure 7(c), there is no significant bond slip between the laminated bamboo beam and BFRP bar, which proves that the once-forming method adopted in this paper is effective. In Figure 7(d), the surface of the BFRP bar became relatively fuzzy and some fibers were fractured. This phenomenon demonstrated that the BFRP bar sustained some part of the force during the test.

Second series: Similar to specimens tested in the first series, the deflection of the reconstituted bamboo beam slowly increased with the increasing load at the initial loading stage but the deflection of the reconstituted bamboo beam developed quickly after the proportional limit for all specimens in the second series. At the ultimate load, the bamboo fibers at the bottom of the beam locally fractured, accompanied with a loud noise. The failure photos, including the overall view and local view, for specimens B0, B1, and B2 in the second series are shown in Figure 8. The failure of the reconstituted bamboo beam with BFRP bar generally initiated around the middle of the beam, and then propagated along the height of the bamboo beam. The failure mode of the three specimens B0, B1, and B2 is characteristic as the fracture of the bamboo fibers in the tensile region. As shown in Figure 9, even if the prestressed force was applied to the BFRP bar, the bond slip between the reconstituted bamboo beam and BFRP bar was avoided. The design of the test specimens was proved to be correct in terms of experimental observations.

4.2. Load–Deflection Relationship. The load versus mid-span deflection curves of specimens A0 and A1, specimens B0, B1, and B2 are shown in Figures 10(a) and 10(b), respectively. The initial anti-arch deflection was considered in Figure 10(b). However, the displacement transducers in the second series deviated from the original positions, making the data after failure cannot be used. To avoid this phenomenon, the noncontact measurement device should be adopted.

First series: As shown in Figure 10(a), the load almost linearly increased with the increasing mid-span deflection at the initial loading stage. When the load increased up to the proportional limit, the laminated bamboo beam entered the plastic state and the relationship between the load and mid-span deflection became nonlinear. Before the failure of the laminated bamboo beam, the deflection has developed to a certain extent. It can be seen that both of the pure laminated bamboo beam and laminated bamboo beam applied with BFRP bar had a good deformation capacity, which promised a good energy dissipation ability. Compared with the specimen A0 (pure laminated bamboo beam), the ductility of the specimen A1 was increased with the existence of the BFRP bar. This phenomenon can be explained as follows: After the ultimate load, the BFRP bar in the specimen A1

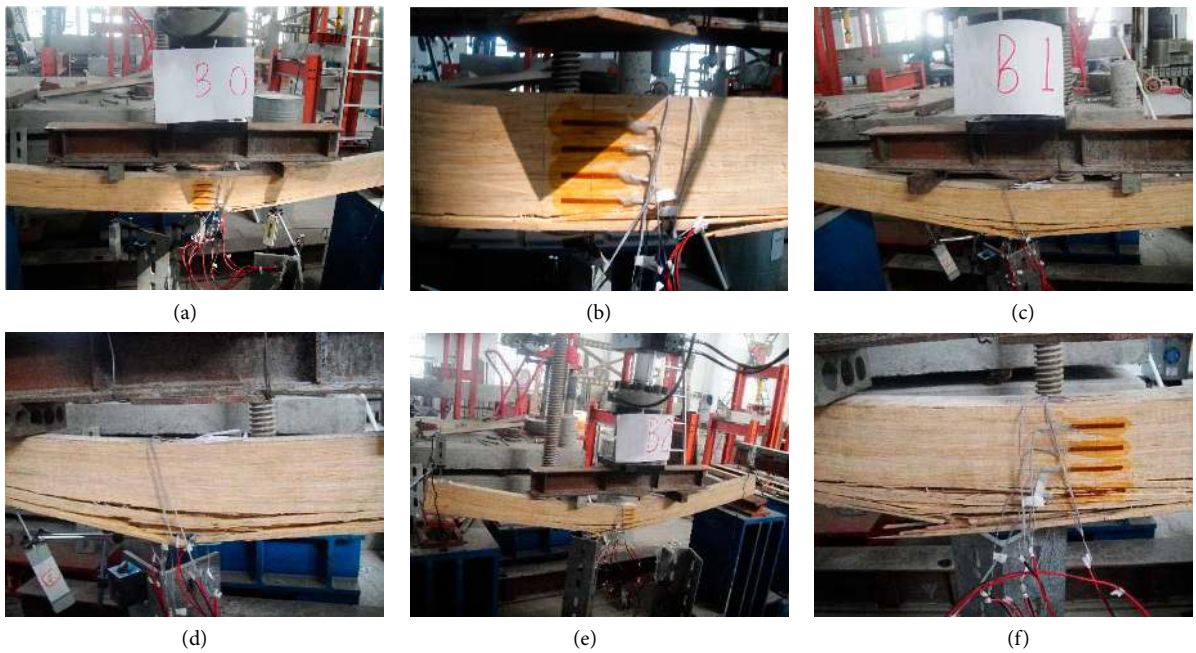

Figure 8: Failure photos for the second series: specimen B0: (a) overall view of, and (b) local view; specimen B1 (c) overall view and (d) local view; specimen B1 (e) overall view, and (f) local view.

Figure 9: Ends of specimens in the second series after loaded: (a) specimen B0, (b) specimen B1, and (c) specimen B2.

could still sustain some part of the load, making the failure of the specimen A1 more ductile compared with the sudden failure of the specimen A0. However, the failure of specimen A1 initiated near the loading point and the crack propagated along the BFRP bar, as shown in Figure 7(b). The failure of specimen A1 was not caused by the fracture of BFRP bar but still the facture of bamboo fibers. The tensile property of the BFRP bar was not fully utilized, which resulted in a limited improvement in the ductility.

The ultimate loads of the specimens A0 and A1 were 9.76 kN and 10.96 kN, respectively. It is obvious that the application of the BFRP bar in the laminated bamboo beam could increase the baring capacity of the laminated bamboo beam. This phenomenon can be explained as follows based on the above experimental observations: The pure laminated bamboo beam could not resist any more load and failed quickly after the ultimate load. However, the BFRP bar participated in the force transfer of the laminated bamboo beam applied with BFRP bar, providing extra bearing capacity. As shown in Figure 10(a), the stiffness of the two specimens was almost the same at the initial loading stage. With the further increase of the load, the stiffness of the specimen A1 became larger than that of the specimen A0.

Second series: Similar to the specimens in the first series, the load linearly increased with the mid-span deflection until the proportional limit in the second series. Then, the specimen entered the nonlinear stage which meant that the deflection developed faster than the load. It is found that the reconstituted bamboo beam applied with prestressed bamboo also had good deformation capacity. Compared with the specimen B0, the mid-span deflections at the ultimate loads of specimens B1 and B2 were a little bit larger.

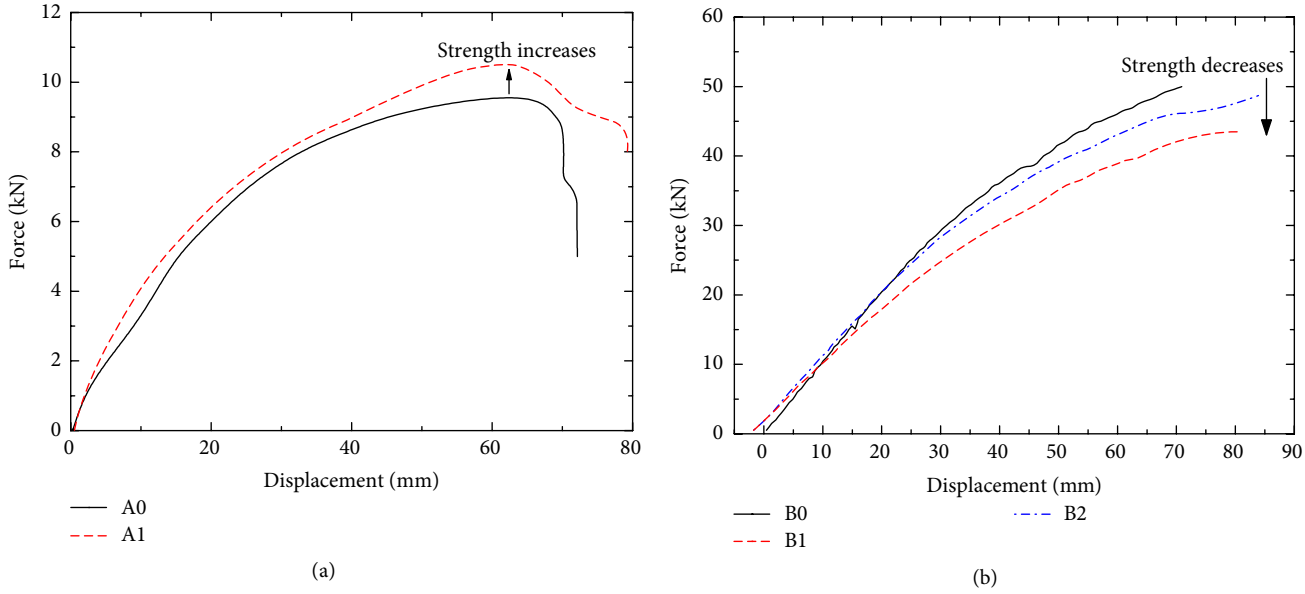

Figure 10: Load–deflection curves at the midspan: (a) first series, and (b) second series.

The ultimate loads of the specimens B0, B1, and B2 were 50.0 kN, 43.5 kN, and 48.5 kN, respectively. The observed difference in the ultimate loads of specimens B0, B1, and B2 was mainly caused by the different dimensions of the three specimens due to fabrication errors. However, the prestressed force would not improve the ultimate load of the bamboo beam. In terms of the ultimate load, the similar variation was found by Borri et al. [42] where the ultimate load of the wood beam was not affected by the application of the prestressed bonded-in FRP bar. As shown in Figure 10(b), no matter whether the initial prestressed force was adopted in the reconstituted bamboo beam, the stiffness would not be changed, which a relevant parameter to the specimen dimension. The slight difference in the initial stiffness of three specimens was also caused by different dimensions.

4.3. Strain Distribution Along Beam Height and Position of Neutral Axis. The strain distributions along the beam height can be captured by strain gages Y-2, Y-3, and Y-4 attached to specimens A0 and A1 and strain gages Y-3, Y-4, Y-5, and Y-6 attached to specimens B0, B1, and B2, which are shown in Figure 11 based on different loads. The abscissa of the figure is the measured strain value and the ordinate is the distance between the strain gage and bottom surface of the beam. An almost linear strain distribution along the beam height at the midspan can be obviously found for the whole loading history. Therefore, the plane section assumption is acceptable for all specimens, including the pure laminated bamboo beam, laminated bamboo beam with BFRP bar and reconstituted bamboo beams with nonprestressed/prestressed BFRP bar.

Based on the detected strain values in Figure 11, the positions of the neutral axis at the midspan under different loads are calculated and listed in Tables 4 and 5 for the two series of specimens. As shown in Table 4, the position of the neutral axis of both specimens A0 and A1 gradually moved down with the increase of the load. Compared with specimen A0 without BFRP bar, the neutral axis of the specimen A1 was lower under the same load. This phenomenon can be explained as follows: As show in Figure 10(a), the applied load of the specimen A1 was larger than that of the specimen A0 under the same

Table 4: Positions of neutral axis under different loads in the first series.

Load (kN)	A0		A1	
	h_l (mm)	h_l/h	h_l (mm)	h_l/h
2	32.70	0.545	22.14	0.369
4	32.22	0.537	23.04	0.384
6	31.26	0.521	23.22	0.387
8	29.64	0.494	21.78	0.363
10	28.08	0.468	18.24	0.304

Note: h_l is the distance between the neutral axis and the bottom surface of the bamboo beam; h is the beam height.

Table 5: Positions of neutral axis under different loads in the second series.

Load (kN)	B0		B1		B2	
	h_l (mm)	h_l/h	h_l (mm)	h_l/h	h_l (mm)	h_l/h
5	65.49	0.543	55.08	0.490	56.53	0.499
10	63.71	0.528	54.87	0.488	56.57	0.499
25	62.69	0.519	53.63	0.477	55.57	0.490
35	59.98	0.497	49.73	0.442	51.52	0.454
45 (40)	55.82	0.462	47.96	0.426	47.23	0.416
P_u	53.61	0.444	46.92	0.417	47.91	0.422

Note: the number in the brackets is for the specimen B1; P_u is the ultimate load.

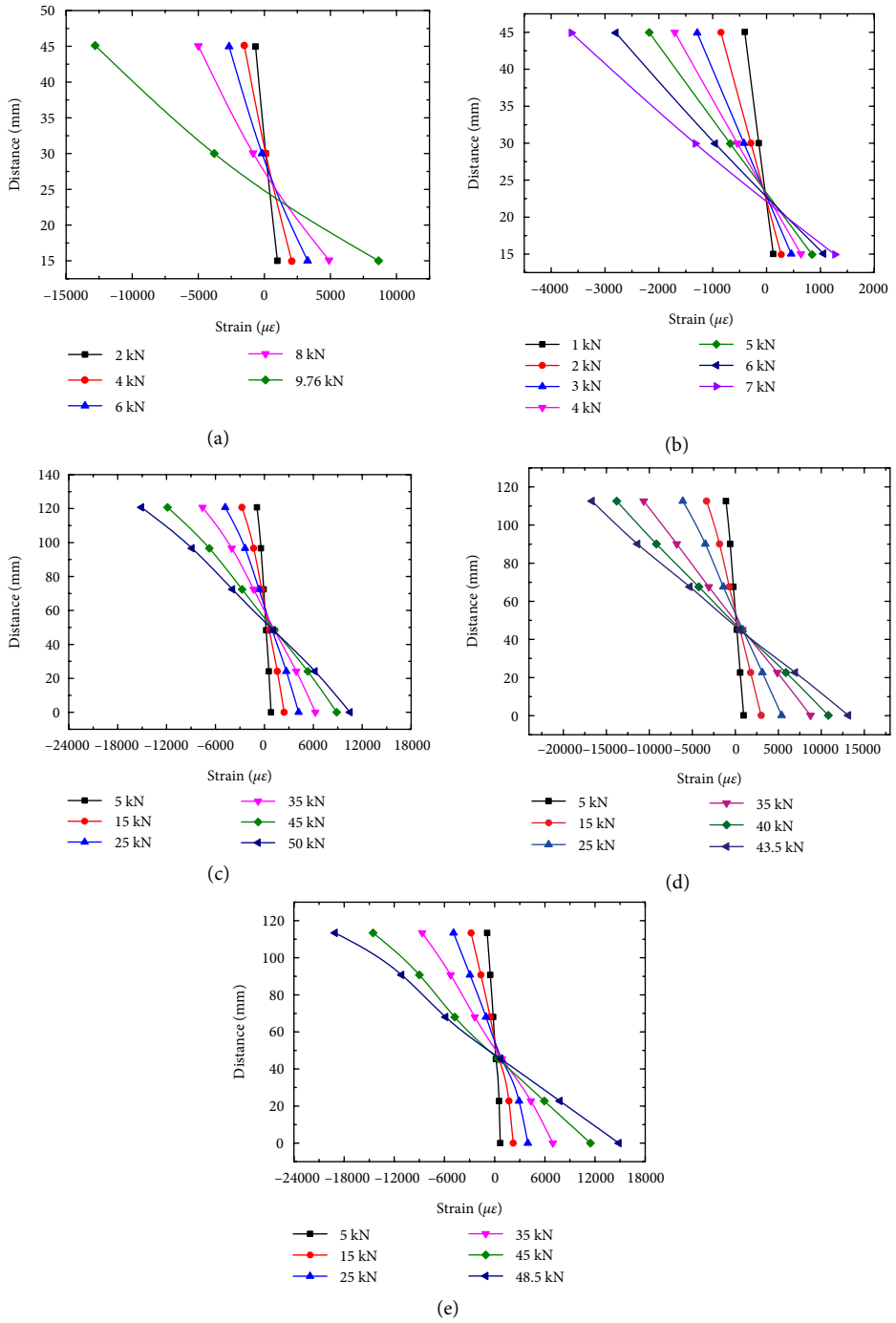

FIGURE 11: Strain distributions along beam height under different loads: (a) A0, (b) A1, (c) B0, (d) B1, and (e) B2.

mid-span deflection due to the existence of the BFRP bar, which demonstrated a higher mid-span cross-section moment in the specimen A1. Based on the force equivalent in the mid-span cross section, the compressive force resisted by part of the bamboo beam' cross section was thus increased, which finally resulted in an increased height of the compression zone. Until the ultimate load, the neutral axes of the specimens A0 and A1 were around 0.468 and 0.304 of the bamboo beam height, respectively.

As listed in Table 5, the neutral axes of the three specimens B0, B1, and B2 stayed almost unchanged at the initial loading stage (less than 10 kN). Then, the neutral axes of the three specimens gradually went down with the further increase of the load. Compared with specimen B0 with nonprestressed BFRP bar, the specimens B1 and B2 applied with prestressed BFRP bar had a relatively similar ratio of h_l/h. This phenomenon was explained as follows: the measurement of the strain values started from the initiation of the loading because the

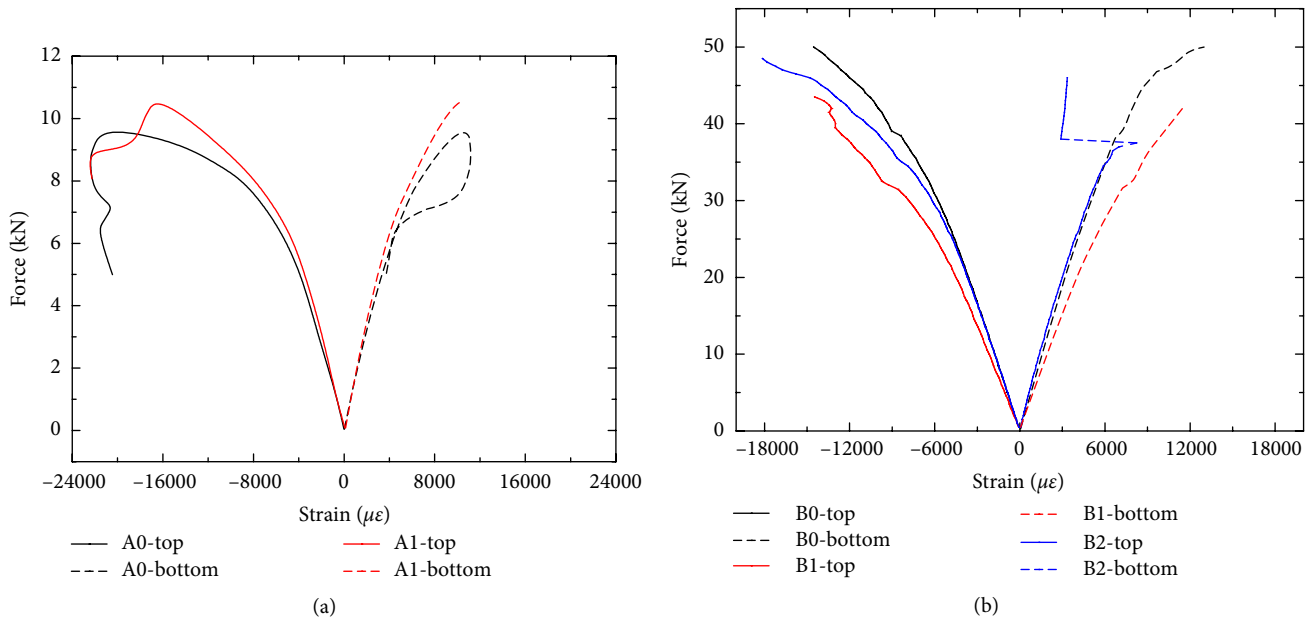

Figure 12: Load–strain curves: (a) first series and (b) second series.

strain cannot be detected during the once-forming fabrication of the reconstituted bamboo beam applied with prestressed BFRP bar in the factory. The effect of the initial strains of the reconstituted bamboo beam and BFRP bar is not considered in the present study, which makes the similar calculated height of the neutral axes of specimens B0, B1, and B2.

4.4. Load–Strain Curves. The load–strain curves of all tested specimens are shown in Figure 12. The data obtained from strain gages Y-1 and Y-5, respectively, monitored the strain variation of the top beam surface and bottom beam surface in specimens A0 and A1, as shown in Figure 6(a). As depicted in Figure 6(b), the strain variation of the top beam surface and bottom beam surface in specimens B0, B1, and B2 was evaluated by the average strain values obtained strain gages Y-1, Y-2 attached on the top beam surface and strain gages Y-7, Y-8 at the bottom beam surface respectively. In general, the maximum compressive strain was larger than the maximum tensile strain for all specimens. The failure of all specimens was explained as the tensile strain of the specimen reached the maximum tensile strain.

It is obvious that the linear strain variation can be observed in all specimen of both series at the initial loading stage. This phenomenon accorded well with the elastic range of the load versus midspan deflection curves at the initial stage discussed in Section 4.2. As shown in Figure 12(a), the compressive strain in the specimen A0 without BFRP bar was larger than the that in the specimen A1 applied with BFRP bar under the same load. A similar law can be found for the tensile strain in specimens A0 and A1.

5. Prestress Loss in the Reconstituted Bamboo Beam Applied with Prestressed BFRP Bar

5.1. Definition of Prestress Loss. During the fabrication of the reconstituted bamboo beam applied with prestressed BFRP bar, types of the prestress loss are summarized as follows: (1) σ_{l1} caused by the deformation of the tensioning equipment and the retraction of the BFRP bar due to tightening of the anchor bolt; (2) σ_{l2} caused by the bond slip between the tensioning fixture and BFRP bar; (3) σ_{l3} caused by the relaxation of the BFRP bar after reaching the target initial prestressed force and before the release of the BFRP bar; (4) σ_{l4} caused by the elastic deformation of the reconstituted bamboo beam at the time of the release of BFRP bar.

5.2. Measurement of Prestress Loss. As mentioned before, the fabrication of the reconstituted bamboo beam was conducted in the factory. It is difficult to monitor the variation of the prestressed force through strain values; and therefore, the prestress loss was only quantitatively measured by the measured anti-arch deflection after the completion of the specimen. The ratio of the total prestress loss of σ_{l1}, $\sigma_{l2,}$ and σ_{l3} to the theoretical initial prestressed stress, η, can be evaluated by the difference between the theoretical anti-arch deflection, ω_0, and measured anti-arch deflection, ω', before the release of the BFRP bar, as expressed in equation (4).

$$\eta = \frac{\sigma_0 - \sigma'}{\sigma_0} = \frac{\sigma_0 - \sigma_0(\omega'/\omega_0)}{\sigma_0} = \frac{\omega_0 - \omega'}{\omega_0}, \tag{4}$$

where σ_0 is theoretical initial prestressed stress caused by F_i; σ' is prestressed stress caused by $F^{'}$ and $F^{'}$ is the actual initial prestressed force considering the prestress loss of σ_{l1}, σ_{l2}, and σ_{l3} before the release of the BFRP bar. Based on Eq. (1) and the plane section assumption, the elastic deformation caused by the actual initial prestressed force $F^{'}$ is calculated in equations (5) and (6).

$$\omega' = \frac{M' l^2}{8EI}, \tag{5}$$

$$M' = \frac{\sigma_{l4} I}{y}, \tag{6}$$

Table 6: Measurement and calculation for the prestress loss.

Label	F_i (kN)	σ_0 (MPa)	ω_0 (mm)	ω' (mm)	$\sigma_{l1}+\sigma_{l2}+\sigma_{l3}$ (MPa)	η	σ_{l4} (MPa)	γ
B1	18.29	161.7	3.14	2.14	51.4	31.8%	5.73	3.54%
B2	16.73	147.9	2.87	1.80	55.2	37.3%	5.25	3.55%

Note: the value of y is estimated as $h/2$ in the calculation of σ_{l4}; γ is the ratio of σ_{l4} to σ_0.

where M' is the cross-section moment caused by the prestress loss σ_{l4}. Thus, the calculation of σ_{l4} is expressed as follows based on equations (5) and (6):

$$\sigma_{l4} = \frac{8\omega' Ey}{l^2}, \tag{7}$$

where y is the distance between the neutral axis and axis of the BFRP bar.

The measurement and calculation of the prestress loss are listed in Table 6. It is found that the decrease of the initial prestressed force caused by the prestress loss ofσ_{l1}, σ_{l2} and σ_{l3} ranged from 31.8% to 37.3% in the present study. The reduction of the initial prestressed force resulted from σ_{l4} was around 3.55% of the theoretical initial prestressed force. Compared with σ_{l4}, the prestress loss of σ_{l1}, σ_{l2} and σ_{l3} had a more significant effect on the initial prestressed force.

5.3. Effective Prestressed Force. Based on the analysis above, the effective prestress, σ_{pe}, can be achieved by subtracting the total prestress loss, σ_l, from the design initial prestressed force, σ_{con}, which is specified as follows:

$$\begin{aligned}\sigma_{pe} &= \sigma_{con} - \sigma_l = \sigma_{con} - \left(\sigma_{l1} + \sigma_{l2} + \sigma_{l3} + \sigma_{l4}\right) \\ &= \sigma_{con}\frac{\omega'}{\omega_0} - \frac{8\omega' Ey}{L_t^2},\end{aligned} \tag{8}$$

where σ_l includes σ_{l1}, σ_{l2}, σ_{l3} and σ_{l4}. Furthermore, the expression of the effective prestress can be simplified as follows:

$$\sigma_{pe} = \sigma_{con}(1 - \eta - \gamma). \tag{9}$$

6. Conclusions

In this paper, the difference in the flexural performance between the pure laminated bamboo beam and laminated bamboo beam applied with nonprestressed BFRP bar and between the reconstituted bamboo beams applied with nonprestressed BFRP bar and prestressed BFRP bar was discussed. Two series of four-point bending tests were conducted in the present experimental program. Main conclusions are summarized as follows:

(1) Based on test results of the first series, it is found that the ultimate load of the laminated bamboo was increased by the application of the nonprestressed BFRP bar. The stiffness of the laminated bamboo beam was relatively improved in the nonlinear stage. In the second series, the ultimate load of the reconstituted bamboo beam was found not to be improved by the application of the prestressed force. The stiffness of the reconstituted bamboo beam was not affected by the initial prestressed force of the BFRP bar in the linear stage.

(2) The design of the application of the initial prestressed force was based on the following principles: avoiding (a) too large initial anti-arch deformation, (b) the bond slip between the bamboo beam and BFRP bar, and (c) the creep fracture of the BFRP bar. The prestress loss before the release of the prestressed BFRP bar accounted for 31.8–37.3% of the design initial prestressed force. Besides, the prestress loss caused by the elastic deformation of the bamboo beam was around 3.55% of the design initial prestressed stress. The calculation method of the effective initial prestressed stress was thus proposed based on the analysis of prestress loss.

(3) The sudden failure of the pure laminated bamboo beam was caused by the fracture of the bamboo fibers while the relatively ductile failure of the laminated bamboo beam applied with BFRP bar was delayed due to the existence of the BFRP bar. The employment of the prestressed force did not have significant effect on the failure mode of the reconstituted bamboo beam.

(4) Based on the strain analysis along the beam height, the plane section assumption was found to be suitable to both of the laminated bamboo beam and reconstituted bamboo beam. The neutral axes of all specimens gradually went down with the further increase of the load.

Data Availability

All data used to support the findings of this study are available from the corresponding author upon request.

Conflicts of Interest

The authors declare that they have no conflicts of interest.

Acknowledgments

The authors would like to acknowledge financial support from the National Natural Research and Development Fund (9Z05000049D0) and Integrated Key Precast Components and New Wood-bamboo Composite Structure (2017YFC0703502).

References

[1] Y. Xiao, Q. Zhou, and B. O. Shan, "Design and construction of modern bamboo bridges," *Journal of Bridge Engineering*, vol. 15, no. 5, pp. 533–541, 2010.

[2] E.-S. Chele, M.-C. Ricardo, P.-M. Ana, and M.-R. Teresa, "Bamboo, from traditional crafts to contemporary design and architecture," *Procedia-Social and Behavioral Sciences*, vol. 51, pp. 777–781, 2012.

[3] J. M. O. Scurlock, D. C. Dayton, and B. Hames, "Bamboo: an overlooked biomass resource?," *Biomass and Bioenergy*, vol. 19, no. 4, pp. 229–244, 2000.

[4] N. Ş. Güçhan, "Observations on earthquake resistance of traditional timber-framed houses in Turkey," *Building and Environment*, vol. 42, no. 2, pp. 840–851, 2007.

[5] Q. Chun, K. V. Balen, and J. Pan, "Flexural performance of small fir and pine timber beams strengthened with near-surface mounted carbon-fiber-reinforced polymer (NSM CFRP) plates and rods," *International Journal of Architectural Heritage*, vol. 10, no. 1, pp. 106–117, 2016.

[6] I. Glišović, B. Stevanović, and M. Petrović, "Bending behaviour of glulam beams reinforced with carbon FRP plates," *Journal of Civil Engineering and Management*, vol. 21, no. 7, pp. 923–932, 2015.

[7] B. Sharma, A. Gatóo, M. Bock, and M. Ramage, "Engineered bamboo for structural applications," *Construction and Building Materials*, vol. 81, pp. 66–73, 2015.

[8] B. Sharma, A. Gatóo, and M. H. Ramage, "Effect of processing methods on the mechanical properties of engineered bamboo," *Construction and Building Materials*, vol. 83, pp. 95–101, 2015.

[9] M. Waite, "Sustainable textiles: the role of bamboo and a comparison of bamboo textile properties-Part 1," *Journal of Textile and Apparel Technology and Management*, vol. 6, no. 2, 2009.

[10] T. Afrin, R. K. Kanwar, X. Wang, and T. Tsuzuki, "Properties of bamboo fibres produced using an environmentally benign method," *The Journal of The Textile Institute*, vol. 105, no. 12, pp. 1293–1299, 2014.

[11] C. J. Lee and J. Park, "Growth model of bamboo-shaped carbon nanotubes by thermal chemical vapor deposition," *Applied Physics Letters*, vol. 77, no. 21, pp. 3397–3399, 2000.

[12] B. Shan, L. Gao, Z. Li, Y. Xiao, and Z. Wang, "Research and applicant of solar energy-prefabricated bamboo pole house," *in Proceedings of the 12th International Symposium on Structural Engineering*, pp. 789–794, 2012.

[13] C. Uko and N. Gowripalan, "Strength properties of raffia bamboo," *Construction and Building Materials*, vol. 3, no. 1, pp. 49–52, 1989.

[14] S. K. Paudel and M. Lobovikov, "Bamboo housing: market potential for low-income groups," *Journal of Bamboo and Rattan*, vol. 2, no. 4, pp. 381–396, 2003.

[15] P. Dua, S. Satya, K. K. Pant, and S. N. Naik, "Eco-friendly preservation of bamboo species: traditional to modern techniques," *BioResources*, vol. 11, no. 4, pp. 10604–10624, 2016.

[16] N. Nugroho and N. Ando, "Development of structural composite products made from bamboo II: fundamental properties of laminated bamboo lumber," *Journal of Wood Science*, vol. 47, no. 3, pp. 237–242, 2001.

[17] M. Mahdavi, P. I. Clouston, and S. R. Arwade, "A low-technology approach toward fabrication of laminated bamboo lumber," *Construction and Building Materials*, vol. 29, pp. 257–262, 2012.

[18] L. Qin and W. J. Yu, "Research on surface color, properties of thermo-treated reconstituted bamboo lumber after artificial weathering test," *Advanced Materials Research*, vol. 79-82, pp. 1395–1398, 2009.

[19] Y. W.-J. Y. Yang-lun and Z. Y. R. Ding-hua, "Studies on factors influencing properties of reconstituted engineering timber made from small-sized bamboo," *China Forest Products Industry*, vol. 6, p. 007, 2006.

[20] W. Yang, J. Shenxue, L. Qingfang, Z. Qisheng, W. Libin, and L. Zhitao, "Experimental study on flexural performance of bamboo beams," *Building Structure*, vol. 1, 2010.

[21] V. De Luca and C. Marano, "Prestressed glulam timbers reinforced with steel bars," *Construction and Building Materials*, vol. 30, pp. 206–217, 2012.

[22] A. Borri and M. Corradi, "Strengthening of timber beams with high strength steel cords," *Composites Part B: Engineering*, vol. 42, no. 6, pp. 1480–1491, 2011.

[23] K. U. Schober and K. Rautenstrauch, "Post-strengthening of timber structures with CFRP's," *Materials and Structures*, vol. 40, no. 1, pp. 27–35, 2007.

[24] Y. J. Kim and K. A. Harries, "Modeling of timber beams strengthened with various CFRP composites," *Engineering Structures*, vol. 32, no. 10, pp. 3225–3234, 2010.

[25] Y.-F. Li, Y.-M. Xie, and M.-J. Tsai, "Enhancement of the flexural performance of retrofitted wood beams using CFRP composite sheets," *Construction and Building Materials*, vol. 23, no. 1, pp. 411–422, 2009.

[26] Y. Nadir, P. Nagarajan, and M. Ameen, "Flexural stiffness and strength enhancement of horizontally glued laminated wood beams with GFRP and CFRP composite sheets," *Construction and Building Materials*, vol. 112, pp. 547–555, 2016.

[27] H. Johnsson, T. Blanksvärd, and A. Carolin, "Glulam members strengthened by carbon fibre reinforcement," *Materials and Structures*, vol. 40, no. 1, pp. 47–56, 2007.

[28] J. Peterson, "Wood beams prestressed with bonded tension elements," *Journal of the Structural Division*, vol. 91, no. 1, pp. 103–120, 1965.

[29] Y. Wei, X. Ji, M. Duan, and G. Li, "Flexural performance of bamboo scrimber beams strengthened with fiber-reinforced polymer," *Construction and Building Materials*, vol. 142, pp. 66–82, 2017.

[30] P. Banibayat and A. Patnaik, "Variability of mechanical properties of basalt fiber reinforced polymer bars manufactured by wet-layup method," *Materials & Design (1980-2015)*, vol. 56, pp. 898–906, 2014.

[31] C. Gentile, D. Svecova, and S. H. Rizkalla, "Timber beams strengthened with GFRP bars: development and applications," *Journal of Composites for Construction*, vol. 6, no. 1, pp. 11–20, 2002.

[32] Q. Lv, Y. Liu, and Y. Ding, "Analyses on prestress loss and flexural performance of the laminated bamboo beam applied with prestressed bfrp sheet," *Advances in Civil Engineering*, vol. 2019, Article ID 2319814, 13 pages, 2019.

[33] Method of Testing in Tensile Strength Parallel to Grain Of Wood (GB/T1938-2009), "State administration of quality supervision, inspection and quarantine," China, 2009.

[34] Method of testing in compressive strength parallel to grain of wood (GB/T1938-2009), "State administration of quality supervision, inspection and quarantine," China, 2009.

[35] D. L. De Lorenzis, V. Scialpi, and A. La Tegola, "Analytical and experimental study on bonded-in CFRP bars in glulam timber," *Composites Part B: Engineering*, vol. 36, no. 4, pp. 279–289, 2005.

[36] J. Sena-Cruz, J. Branco, M. Jorge, J. A. O. Barros, C. Silva, and V. M. C. F. Cunha, "Bond behavior between glulam and GFRP's

by pullout tests," *Composites Part B: Engineering*, vol. 43, no. 3, pp. 1045–1055, 2012.

[37] M. Madhoushi and M. P. Ansell, "Experimental study of static and fatigue strengths of pultruded GFRP rods bonded into LVL and glulam," *International Journal of Adhesion and Adhesives*, vol. 24, no. 4, pp. 319–325, 2004.

[38] Q. Lv, Y. Liu, and Y. Ding, "Study on bond behaviors between BFRP bar/sheet and bamboo engineering materials," *Advances in Structural Engineering*, vol. 22, no. 14, pp. 3121–3133, 2019.

[39] X. Wang, J. Shi, J. Liu, L. Yang, and Z. Wu, "Creep behavior of basalt fiber reinforced polymer tendons for prestressing application," *Materials & Design*, vol. 59, pp. 558–564, 2014.

[40] C. P. Press, *Technical Code for Infrastructure Application of FRP Composites, GB-50608*, Beijing, 2010.

[41] X. Wang, J. Shi, G. Wu, L. Yang, and Z. Wu, "Effectiveness of basalt FRP tendons for strengthening of RC beams through the external prestressing technique," *Engineering Structures*, vol. 101, pp. 34–44, 2015.

[42] A. Borri, M. Corradi, and A. Grazini, "A method for flexural reinforcement of old wood beams with CFRP materials," *Composites Part B: Engineering*, vol. 36, no. 2, pp. 143–153, 2005.